Received: 3 June 2021 | Revised: 24 September 2021 | Accepted: 24 October 2021

DOI: 10.1111/cbdd.13978

RESEARCH ARTICLE

WILEY

Specific delivering of RNAi using Spike's aptamer-functionalized lipid nanoparticles for targeting SARS-CoV-2: A strong anti-Covid drug in a clinical case study

Haidar Saify Nabiabad[1] | **Massoume Amini**[1] | **Serwet Demirdas**[2]

[1]Department of Biotechnology, Bu-Ali Sina University, Hamadan, Iran

[2]Department of Clinical Genetics, Erasmus Medical Centre, Rotterdam, the Netherlands

Correspondence
Haidar Saify Nabiabad, Department of Biotechnology, Bu-Ali Sina University, Hamadan, Iran.
Email: homan_saify@yahoo.com

Abstract

Coronavirus (SARS-CoV-2) as a global pandemic has attracted the attention of many scientific centers to find the right treatment. We expressed and purified the recombinant receptor-binding domain (RBD) of the SARS-CoV-2 spike (S) protein, and specific RBD aptamers were designed using SELEX method. RNAi targeting nucleocapsid phosphoprotein was synthesized and human lung cells were inoculated with aptamer-functionalized lipid nanoparticles (LNPs) containing RNAi. The results demonstrated that RBD aptamer having K_D values of 0.290 nM possessed good affinity. Based on molecular docking and efficacy prediction analysis, siRNA molecule was showed the best action. LNPs were appropriately functionalized by aptamer and contained RNAi molecules. Antiviral assay using q-PCR and ELISA demonstrated that LNP functionalized with 35 μM Apt and containing 30 nM RNAi/ml of cell culture had the best antiviral activity compared to other concentrations. Applied aptamer in the nanocarrier has two important functions. First, it can deliver the drug (RNAi) to the surface of epithelial cells. Second, by binding to the SARS-CoV-2 spike protein, it inhibits the virus entrance into cells. Our data reveal an interaction between the aptamer and the virus, and RNAi targeted the virus RNA. CT scan and the clinical laboratory tests in a clinical case study, a 36-year old man who presented with severe SARS-CoV-2, demonstrated that inhalation of 10 mg Apt-LNPs-RNAi nebulized/day for six days resulted in an improvement in consolidation and ground-glass opacity in lungs on the sixth day of treatment. Our findings suggest the treatment of SARS-CoV-2 infection through inhalation of Aptamer-LNPs-RNAi.

KEYWORDS

antiviral, aptamer, inhalation, lipid nanoparticles, RNAi, SARS-CoV-2

Abbreviations: Apt, aptamer; DMKE, *O,O′*-Dimyristyl-N-lysyl glutamate; DSPE-PEG2000, 1,2-distearoyl-sn-glycero-3-phosphoethanolamine-N-[methoxy(polyethylene glycol)-2000] (ammonium salt); ELISA, enzyme-linked immunosorbent assay; HRP, horseradish peroxidase; KD, dissociation constant; LNPs, lipid nanoparticles; PEG, polyethylene glycol; RBD, receptor-binding domain; RISC, RNA-induced silencing complex; RNAi, RNA interference; SARS-CoV-2, novel coronavirus. ACE2, angiotensin-converting enzyme II; SARS-CoV-2, Severe acute respiratory syndrome coronavirus 2; SELEX, Systemic Evolution of Ligands by EXponetial enrichment; carbon nanotubes; ssDNA, single-stranded DNA; TBST, Tris buffer saline Tween-20; TMB, 3,3′,5,5′-tetramethyl benzidine.

1 | INTRODUCTION

The coronavirus-2019 (SARS-CoV-2) is spreading rapidly around the world and leading to millions of deaths. SARS-CoV-2 is enveloped positive ssRNA viruses having four structural proteins; membrane (M), spike glycoprotein (S), envelope (E), and nucleocapsid phosphoprotein (N) that facilitate interactions with the host cell (Westerbeck & Machamer, 2019). Coronaviruses can cause several illnesses including gastroenteritis and respiratory tract infections. In severe cases, patient dies due to progressive respiratory failure and massive alveolar damage (Chan et al., 2020; Song et al., 2020). The spike glycoprotein of SARS-CoV-2 binds directly to angiotensin-converting enzyme II (ACE2) receptor through the receptor-binding domain (RBD) in the S1 subunit facilitating virus entry into alveolar epithelial cells of lung (Walls et al., 2016 and Zhou et al., 2020). This makes the RBD of the SARS-CoV-2 spike protein a key candidate for the diagnosis and treatment of SARS-CoV-2 (Song et al., 2021 and Walls et al., 2016). The nucleocapsid is a protein, which packages the SARS-CoV-2 genome and has an important role for viral self-assembly. Post-transcriptional gene silencing by RNA interference (RNAi) is a regulatory cellular mechanism involving small RNAs (about 30 bases) that regulate the gene expression. RNAi is previously reported as a prospective treatment of viral infections (Levanova & Poranen, 2018), and parasites (Chowdhury et al., 2019). RNAi molecule is loaded into the RNA-induced silencing complex (RISC) and argonaute subunit degrades targeted mRNA. Studies show that chemically synthesized siRNA duplexes targeting genomic RNA of SARS-CoV results in therapeutic activity (Zheng et al., 2004 and Lysebetten et al.; 2021). By using RNAi as therapeutic agents, it is possible to reduce or block the production of disease-causing proteins (Cook & Decuzzi, 2021 and Lan et al., 2021). However, naked RNAi molecules cannot effectively pass through the cell membrane due to their high negative charges density (Geng et al., 2020). For SARS-CoV-2, developed RNAi could be given to patients via intranasal delivery, pulmonary route by inhalation and intratracheal aerosol delivery (Youngren et al., 2016). The pulmonary proteases, intense mucus layer, inflammation, and alveolar macrophages are an obstacle for RNAi to attach target cells (Youngren et al., 2016). These restrictions can be mitigated by delivering RNAi molecules using inorganic origin RNAi nanocarrier systems such as lipid-based nanoparticles (Terada et al., 2021).

In this method, RNAi molecules were encapsulated by using lipid-based nanoparticles, which provide more stability and well penetration to target tissue (Ge et al., 2021; Saw & Song, 2019).

Aptamers, single-stranded oligonucleotides that bind to targets such as proteins, as commonly used ligands enable specific recognition and tight binding to receptors that modulate cell fate.

The superiority of aptamers over monoclonal antibodies includes their ease of synthesis, easy chemical modifications, high stability and low immunogenicity. These benefits make aptamers an ideal tool as a therapeutic agent or for targeted delivery (Song et al., 2021).

We investigated to develop a SARS-CoV-2-specific delivery system for antiviral RNAi. First, we expressed and purified SARS-CoV-2 RBDs, synthesized specific RBD aptamer using SELEX method, and designed RNAi specific to SARS-CoV-2 nucleocapsid phosphoprotein. We aimed to synthesis dual-role aptamers that could achieve specific RNAi delivery and bind spike protein to inhibit SARS-CoV-2 entry into cells. We prepared LNPs modified with RBD aptamer and containing RNAi targeting virus nucleocapsid. Finally, anti-SARS-CoV-2 activity of aptamer-functionalized LNPs containing RNAi (Apt-LNPs-RNAi) was investigated in human epithelial lung cells. Our data demonstrate a real SARS-CoV-2–specific delivery system that leads to the inhibition of SARS-CoV-2 at the cellular level.

2 | METHODS AND MATERIALS

2.1 | Expression and purification of recombinant RBD-Spike protein

Viral total RNA was extracted from sputum of SARS-CoV-2 positive patients (confirmed by q-PCR) and cDNA synthesized by means of Kogen extraction kit (Kogen, South Korea). The fragment of the RBD Spike protein (Genbank accession No.: AY687357.1) was amplified from SARS-CoV-2 cDNA by means of a PCR with synthesized primer-oligonucleotides (forward primer: 5′-GGATCCAT GTGTCTATGCATGGGAGAGGA-3′ and reverse primer: 5′-CGAGCTCGTTA TCAGAAACATCACGGCCAAA-3′) containing a stop codon and start codon. Amplified segment was extracted from agarose gel, ligated to the pET-21a vector and transformed into competent *E. coli* DH5α cells. Finally, recombinant RBD Spike protein was purified using chromatography column according to the previous method (Saify Nabiabad et al., 2018).

2.2 | SDS-PAGE and Western blotting to confirm RBD Spike protein

The purified RBD protein was approved by SDS-PAGE and western blotting as described by Saify Nabiabad et al. (2018). Briefly, total protein was separated by 15% Tris-glycine SDS-PAGE (Invitrogen) and stained with Coomassie brilliant blue or transferred to nitrocellulose

membranes. The blots were blocked with 6% fat-free milk in PBS containing 0.6% Tween-20 for 3 h at 38°C and further incubated with SARS-CoV-2 RBD-specific antibody (1:3000. Invitrogen, T01KHu), overnight at 4°C. The blots were then incubated with horseradish peroxidase (HRP)-conjugated IgG (1:5000, Thermo Fisher Scientific) for 1 h at 27°C and then visualized.

2.3 | Aptamer synthesis

2.3.1 | Amplification of single-stranded DNA (ssDNA) library

The applied ssDNA library was 5′ dATCCGGATCC-CGCGC (N22) GCGCTAAGCTTCGCGC-3′ (Bioneer Co. South Korea). The DNA library was amplified using asymmetric PCR and analyzed by electrophoresis. The PCR conditions used were maintained during all selection rounds as follows: 38 cycles of 60 s at 95°C for denaturation, 55 s at 57°C for annealing, and 30 s at 72°C for extension, followed by 6 min at 72°C for final extension. The specific primers were GCGCGAAGCTTGCGC as reverse primer and ATGCGGATCCCGCGC as forward primer, which *HindIII* and *BamHI* restriction sites are underlined, respectively). The PCR product was separated by 12% polyacrylamide gel electrophoresis. The small band DNA, corresponding to the antisense strand amplified by the reverse primer, was purified from the agarose gel.

2.3.2 | Selection of aptamers

The aptamer selection round was performed using a membrane filtration method (30 kDa cutting membrane) under SELEX protocol as shown in Table 2. The purified RBD was incubated with Tris–HCl (pH 8.0) for 40 min, with various concentrations of ssDNA, for various times at 30 °C (Table 2). After incubation, RBD-bound aptamer complexes were centrifuged at 18928 *g* for 12 min for the complete washing of unbound aptamers. The supernatant was discarded and RBD-bound aptamer complexes were washed with 6 mM Tris buffer (pH 8.0). The aptamers, which participated in the formation of the RBD complex were amplified by PCR and extracted from 15% PAGE gel electrophoresis. The eluted ssDNA product from gel was subsequently used for the next round of selection. The negative selection rounds were performed using recombinant Influenza A Virus Nucleoprotein (INP). This process was repeated 9 times with varying conditions, in order to increase the specificity of the aptamer for the target RBD. The enriched aptamer pool was cloned in T/A cloning vector and transformed into competent *E.coli DH5α*. Plasmids from confirmed positive colonies were sequenced and a sequence with the highest frequency were considered as the candidate RBD aptamer.

2.3.3 | Binding affinity and selectivity of RBD aptamers

Aptamer molecules were synthesized and modified with biotin at the 5′ end to evaluate their dissociation constant (KD) using an ELISA test. The KD was calculated from the chemiluminescence intensity based on a nonlinear regression equation. A 5′ biotin-labeled aptamer and a streptavidin horseradish peroxidase (HRP) antibody were used for this method. A fixed concentration of RBD (0.001 mg/well in 100 µl) prepared in TBST buffer (pH 7.4) was loaded onto a polystyrene plate (96-well) and incubated for 1 h at 30°C on a shaker (100 rpm) for immobilization of the RBD. Wells containing RBD were washed with 200 µl TBST three times and incubated with 100 µl of 2% BSA for 1 h. Wells was washed with 1× TBST for five times, and various concentrations of biotinylated aptamer (90 µl) was added to the wells and incubated for 2 h on a shaker (100 rpm). Unbound aptamers were removed by washing TBST, 95 µl streptavidin HRP (1:2500 in TBS) was added to the wells and incubated at room temperature for 1 h on a shaker. After washing the wells for several times with 400 µl TBST, 95 µl TMB substrate solution (3,3′,5,5′-tetramethyl benzidine) was added to each well. Finally, the reaction was stopped by the addition of 95 µl of H_2SO_4 (1 M), followed by the recording of the OD at 450 nm with ELISA reader.

2.4 | Designing of Nucleocapsid phosphoprotein RNAi

RNAi molecules were designed according to method of Chowdhury and Sharif Shohan (2021). Briefly, coding sequences from genomes of SARS-CoV-2 were retrieved from NCBI. Nucleocapsid phosphoprotein sequence was manually extracted and curated from the retrieved data using bash Shell scripting. Multiple sequence alignment was performed using Clustal W algorithm. Nucleocapsid phosphoprotein-specific RNAi was designed using si-Direct web server (siDirect (rnai.jp)). siRNAPred server (http://crdd.osdd.net/raghava/sirnapred/index. html) was used to validate the predicted RNAi species. RNAi modified with 3′-hexylamine on the sense strand, was obtained from Samchunlly Inc.

2.5 | Aptamer-lipid nanoparticle-RNAi preparation

Aptamer-modified LPNs containing RNAi were prepared according to protocol of Kim et al. (2017). DMKE (45% mole), DSPE-PEG2000 (4% mole; Merck) and cholesterol (46% mole; Avanti, Inc) were dissolved in a methanol and chloroform mixture (2:1, v/v). The organic solvent was evaporated using a stream of N2 gas. Dried films containing 2 mg of lipid were hydrated in 2 ml of saline, mixed for 6 min and then sonicated 3 times for 12 min each at 15 min intervals. Then, RNAi molecule (40–80 nM) was added to the prepared liposomes and incubated with vortexing for 30 min at 30°C. Finally, the DSPE-mPEG2000-conjugated aptamers (50–90 μM) were inserted into the prepared LNPs-siRNA by incubating for 3 h at 37°C. The aptamers conjugation and its purity were defined on a 2% agarose gel.

2.6 | Cell culture experiments

An isolate of SARS-CoV-2 (P.1 lineage (a.k.a. 20J/501Y.V3)) was used in this study. Nasopharyngeal sample was obtained after clinical diagnosis with SARS-CoV-2 (Ct value of 18 in q-PCR assay, and positive IgG/IgM after 20 days) and irreversible anonymization. All cell culture protocols were performed based on the method of Ramirez et al., 2020. All initial culture of SARS-CoV-2 was performed in African green monkey kidney cell lines (Vero E6). Vero E6 cell line was obtained from Merck and authenticated by STR markers D5S1467, D17S1304, D19S245, D8S1106, D1S518, D4S2408, D6S1117, and DYS389. For inoculation, 25 μl of the Nasopharyngeal samples were added into Vero E6 cells, and seeded in 12-well plates. Vero E6 cells were cultured in DMEM, supplemented with 12% fetal bovine serum and Antimycotic-Antibiotic (10,000 μg/ml of streptomycin, 10,000 units/ml of penicillin, and 24 μg/ml of Amphotericin B, Gibco) and kept in a humidified incubator with 5% CO2 at 37°C. A SARS-CoV-2 stock was prepared by pooling 10 ml of filtered supernatant (0.45 μM filter) from the samples harvested at day 3 from second passages, and stored at −80°C.

Epithelial lung cancer cell line (HBE135-E6E7) was cultured. HBE135-E6E7 cell line was obtained from ATCC and authenticated by STR markers CSF1PO, D13S317, D16S539, D5S818, D7S820, THO1, TPOX, and vWA. Three subcultures were conducted in HBE135-E6E7. Subcultures were performed by inoculating 0.5 ml of Vero E6 supernatant for subsequent passages. The third passage was carried out in T-175 flasks. To explore the overall antiviral activity of Apt-LNPs-RNAi (drug potency), 50 μl of Apt-LNPs-RNAi (different concentrations as indicated in Figure 5) were added and the cells were incubated for 72 h. After the 72-h incubation, antiviral activity was assessed by ELISA and q-PCR (Saify Nabiabad et al., 2018). Remdesivir (AdooQ BioScience) was used as a positive control in the experiments.

2.7 | Clinical case report

The clinical study was approved by the ethics committee of Rojava University (17/09/2020). Patients, who referred to the SARS-CoV-2 hospital in Rojava and were willing to participate in the study completed the consent forms. Moreover, Patient Consent for Publication was assigned by the patient.

The case study was a 36-year old man, who presented with severe fever, dyspnea, and cough for 3 days and subsequently positive qRT-PCR for SARS-CoV-2. A soft mist inhaler (Respimat®) was used for inhalation of Apt-LNPs-RNAi, so that 10 mg Apt-LNPs-RNAi nebulized/day for six days. Chest computerized tomography (CT) scan and biochemical analysis were performed regularly. The consent form was signed by the patient for blood sampling and CT scan. CT scan images were analyzed by radiologists.

3 | RESULTS

3.1 | Cloning, expression, and protein integrity assay

The SARS-CoV-2 RBD segment was expressed in a fermenter. Results of PCR and sequencing indicated that RBD segment was cloned approximately (Figure 1a). Total protein was extracted from transgenic bacteria and RBD segment purified by nickel chromatography, which elutes were first analyzed by SDS-PAGE (Figure 1c) and finally approved by western blot (Figure 1b). Immunoblotting analysis confirmed the expression of RBD segment (a distinct protein band with the estimated 28 kDa weight) in the purified samples.

3.2 | Selection of aptamers against RBD

High-affinity aptamers directed toward the RBD were selected through nine rounds of DNA-SELEX using the stringent conditions applied during each round of selection (Table 1 and Figure 3b). The incorporation of recombinant Nucleoprotein of Influenza A Virus (INP, Abcam; ab224859) during the negative selection rounds improved the selectivity of the DNA aptamers. Consequently, aptamer molecules that bound the RBD

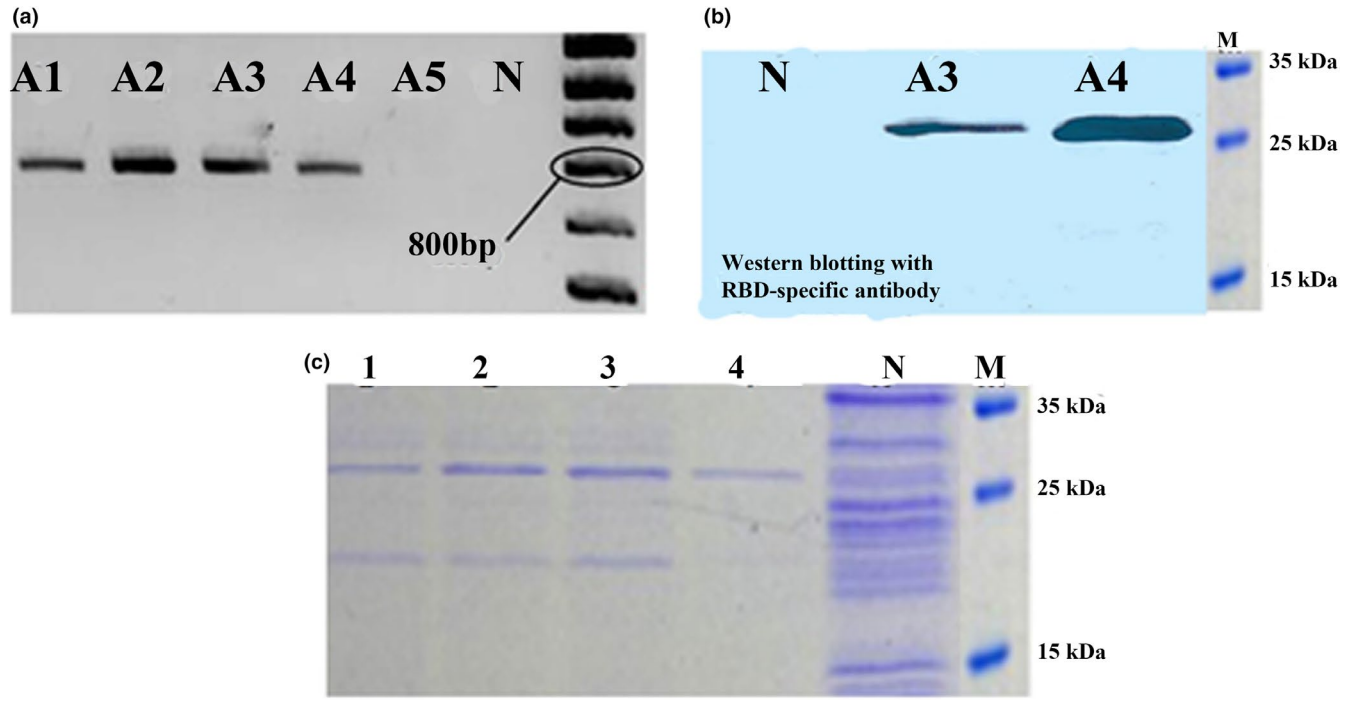

FIGURE 1 Cloning and purification of RBD. (a) RT-PCR that indicated expression of cloned RBD in *E.coli* demonstrated an 800 bp band corresponding to cloned segment of RBD. Line A1-A5 are transformed bacteria and line N is nontransformed one. (b) Western blot analysis of proteins. Lane N: negative control (*E. coli* without RBD), Lane A3, and A4 are purified recombinant RBD. (c) SDS–PAGE of purified recombinant *RBD* via Ni-Sepharose affinity chromatography. Lane 1–4: purified protein from different lines of bacteria demonstrated a 28 kDa protein band corresponding to RBD size, line N: total protein before purification and M is protein ladder [Colour figure can be viewed at wileyonlinelibrary.com]

TABLE 1 Conditions of SELEX for selection aptamers toward RBD

	1	2	3	4	5	6	7	Negative selection	8	9
(Tris Buffer, mM)	25	25	25	40	40	40	50	50	100	100
NaCl	10	10	10	50	50	50	50	50	100	150
Protein (μg)	10	10	10	8	8	8	8	2% INP	5	2
ssDNA library (ng)	500	500	500	400	400	400	400	400	300	200
Incubation time (min)	60	60	60	60	60	60	60	60	45	30

TABLE 2 Sequences of aptamers and their properties

Aptamer	Aptamer sequence (5′→3′)	K_D (μM)	frequency
Apt1	CAGCCACGACCTGTTGCTTTGGGAGTGCTGGTCCAAGGGACGTTATGGACA	0.290 ± 0.07	15/30
Apt2	GCTGGATGTCGCTTACGACAATATTCCTTAGGGGCACCGCTACATTGACAC	0.44 ± 0.05	7/30
Apt3	TGTTCCAAGGTGTGTGGCGGTTGATGTCGCTGCTAGCTACATTCATTGTTG	2.06 ± 0.4	5/30
Apt4	TGTTCCAAGGGGTTGTGTGTGGCATGAGCTACATTTCGCTGCTCATTGTTG	2.26 ± 0.3	3/30

with higher affinity were enriched. The RBD-bound aptamers were eluted by heat denaturation during PCR-amplification and were further amplified, followed by extraction of the PCR products from the gel. After nine rounds of SELEX, the aptamers directed toward the RBD were cloned and sequenced. Sequencing demonstrated that some amplified aptamer molecules dominated the pool (Table 2), and the affinity potential of these repetitive aptamers to RBD was evaluated.

The dissociation constant (K_D, shown in Table 2) represents the binding affinity of the aptamers toward the molecule target. Lower K_D values represented higher

aptamer affinity to RBD. The K_D results demonstrated that Apt1 with K_D values of 0.290 ± 0.07 μM had the highest affinities toward the RBD than the other sequences. In contrast, the negative controls [Influenza A Virus Nucleoprotein (INP)] showed no apparent affinity to Apt1 at concentrations of up to 6 μM. Briefly, the performance of aptamer 1 (Apt1) in RBD recognition and affinity exceeded that of the others. Therefore, Apt1 was regarded as the best candidate aptamer for the next investigations.

3.3 | Designing and selection of siRNA

The phylogenetic tree indicated that most of the SARS-CoV-2 sequences are conserved (Ayal et al., 2020) and could be used to produce siRNA, which cover a large number of SARS-CoV strains. siDirect database (siDirect (rnai.jp)) predicted 5 siRNAs for N protein that maintain all the parameters. Seed target duplex stability (Tm) index for the predicted siRNAs was less than 21.5°C, which suggests the ability of designed siRNAs to avoid nonspecific and nontarget binding. Blast search against transcriptome and human genome did not indicate any off-target match. siRNAPred web (http://crdd.osdd.net/raghava/sirnapred/index. html) checked the effectivity of the predicted siRNAs and values greater than 1 are considered highly effective. One siRNA for N protein was found to be highly effective (Table 3) and advanced for molecular docking.

Guide strand of predicted RNAi was subjected to mRNA structure web (https://rna.urmc.rochester.edu/RNAstructureWeb/Servers/MaxExpect/MaxExpect html Maxexpect) in order to find mRNA-folding structures and minimum free energies. At 37°C, selected RNAi has folding-free energy greater than zero, which indicates the predicted RNAi molecule is more ready for efficient binding. After modeling, molecular docking of the siRNA and Ago2 was done using the HDOCK server (http://hdock.phys.hust.edu.cn/). Hdock server reveals top models of RNAi binding to Ago2 according to docking scores (Figure 2). Some residues, such as ARG315, LYS533, THR526 and ARG277 interacted with RNAi that previously reported (Bhandare & Ramaswamy, 2016).

3.4 | Preparation and characterization of Apt-LNP-RNAi

The synthesis steps for aptamer-coupled liposomes harboring siRNA (Apt-LPN-RNAi) are illustrated in Figure 3a. First, liposomes were prepared by the thin-film hydration and drying method. Next, RNAi molecules were

TABLE 3 Best effective siRNA molecules with various parameters

Conserved position	siRNA target within mRNA	Duplex candidate at 37°C	Predicted siRNA(guide): siRNA (passenger)	Seed duplex (Tm) guide	Tm (Conc)	Validity (binary)
1031-1253	AAGCATATTGCAGCATACAAAAC	GCAUAUGUACGCAUACAAAAC	UUUGUACUGGUCAAUAUGCUU	13	76	1.47
870-1221	CAGAAACAAAGTGTACGTTGAAC	GAAAGAAAGUGUACGUUGAAA	UCAACGUACACCUUGUUUCUG	21	79	1.22
870-1221	TGCCCTTTTGGTGAAGCTTTTAA	CCCGUUUUGGUGAAGUUUUUAA	AAAACCUUCACCAAAAGGGCA	3.3	83	1.04
1841-2388	CACAATTCAACCGTGCTTTAACT	CAAUUCAACCGUGCUUUAACU	UUAAGGCACGGUUUAAUUGUG	19.00	79.01	1.12
2790-3822	GTGTGTACCTGGACAATCAAAAA	GUGUAAUUGGACAAUCAAAAA	UUUGAUUGUCCAAGUCCACAC	13.9	80.3	1.00

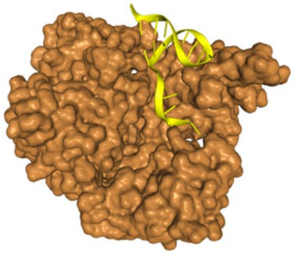

Complex Template Information

Molecule	PDB ID	Chain ID	Align_length	Coverage	Seq_ID (%)
Ligand	2F8S	C	7	0.333	100.0

Summary of the Top 10 Models

Rank	1	2	3	4	5	6	7	8	9	10
Docking Score	-331.85	-301.75	-299.36	-281.00	-280.89	-270.10	-269.85	-265.69	-264.05	-262.36
Ligand rmsd (Å)	91.14	76.77	80.93	105.00	82.14	89.66	79.24	78.64	104.35	99.21

(a) Row 1: The ranks of the models.
(b) Row 2: The docking energy scores.
(c) Row 3: The ligand RMSDs from the input structures or modeled structures by homology modeling.

FIGURE 2 Docking model of Argonaute2 (surface view) with RNAi (cartoon view). The RNAi was designated by yellow color [Colour figure can be viewed at wileyonlinelibrary.com]

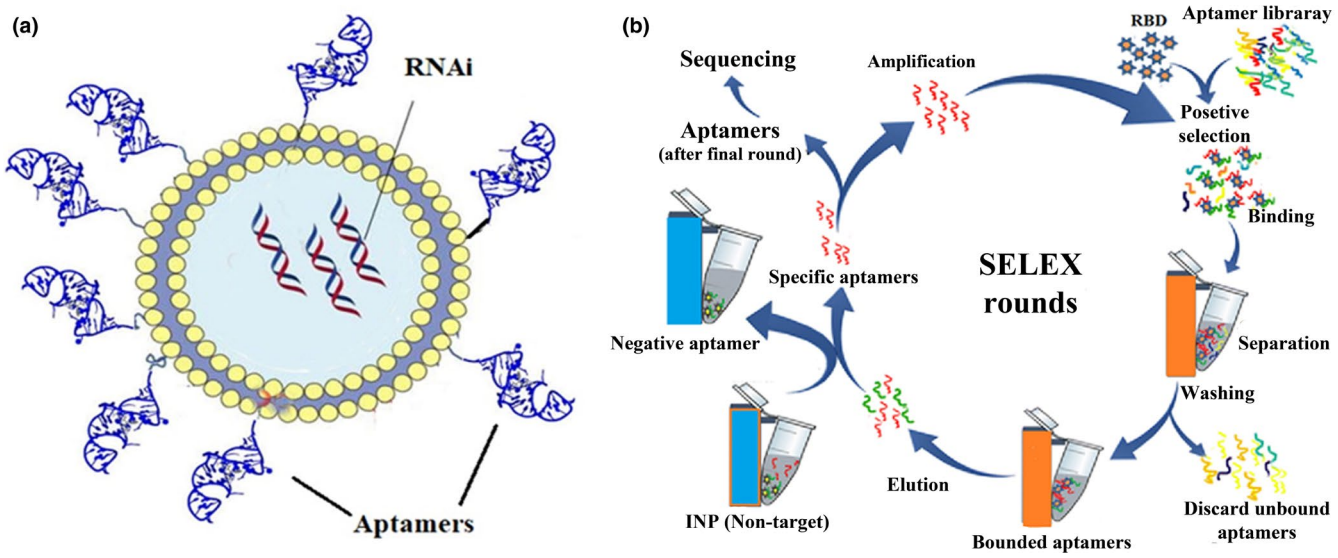

FIGURE 3 (a) Synthesis of Apt-LNPs-RNAi. Lipid nanoparticles were complexed with siRNAs, and the aptamer-DSPEPEG2000 molecules conjugates were then inserted into the LNPs-RNAi to form the Apt-LNPs-RNAi complex. (b) Aptamers selection round against the RBD of the SARS-CoV-2 -spike glycoprotein [Colour figure can be viewed at wileyonlinelibrary.com]

complexed with LNPs by continuous mixing. Presumably, RNAi molecules would preferentially attach or associate with the cationic surface of the LNPs. Then, conjugates made of RBD aptamers and DSPE-PEG2000-MAL, referred to as Apt-DSPE-PEG2000, and additional distearoyl phosphoethanolamine-methylpolyethyleneglycol-2000 (DSPE-mPEG2000) were coupled by the post-insertion method.

Results of gel retardation assay indicated RNAi complexation at N/P ratios varying from 2:1 to 12:1 and confirmed the formation of the siRNA/liposome complex at the N/P ratios of more than 2:1 (Figure 4a). Significant retardation of RNAi molecules due to coupling with cationic lipids was observed at an P/N ratio of 1:6. Digestion of siRNA with RNAse A indicated that Apt-LNPs could effectively protect the incorporated RNAi molecules from cellular endonucleases degradation, leaving 75% of the siRNAs intact (Figure 4b). As shown in Figure 4c, RBD aptamers were efficiently conjugated to DSPE-PEG2000-maleimide, and then aptamer- DSPE-PEG2000 was successfully attached to the prepared liposomes.

3.5 | In vitro anti- SARS-CoV-2 assessment of apt-LNPs-RNAi

SARS-CoV-2 was adapted to efficient growth in lung cell lines (HBE135-E6E7). Vero E6 cells, which permit the isolation of SARS-CoV-2 were used to obtain the initial virus stock. The virus supernatant derived from the Vero E6 passage was used to inoculate lung cell lines. After culture of the virus, the antiviral susceptibility of SARS-CoV-2 for Apt-LNPs-RNAi was determined by measuring the reduction of the SARS-CoV-2 titer in culture supernatants using q-PCR and ELISA. The 50% inhibitory concentration of Apt-LNPs-RNAi was reported as the concentration of antiviral drug that reduced the

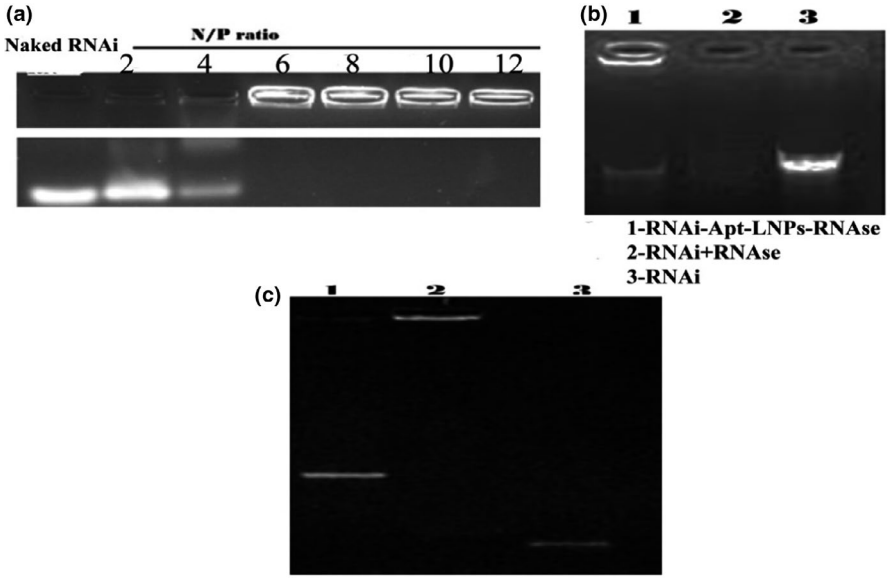

FIGURE 4 Gel retardation assay of Apt-LNPs containing RNAi on a 2% agarose gel. (a) prepared LNPs-siRNAs at different N/P ratios (2:1 to 12:1)were electrophoresed. Significant retardation of siRNA molecules due to coupling with cationic lipids was observed at an N/P ratio of 6:1 (b) Apt-LNPs-RNAi at an N/P ratio of 4:1 were electrophoresed after treatment with RNase A (0.1 mg/ml). Lane 1: Apt-LNPs-RNAi treated by RNAse A, Lane 2: RNase A-treated siRNA; Lane 3: untreated RNAi. (c) aptamer-DSPE-PEG2000 molecules were inserted into the LNPs containing RNAi, which were then electrophoresed. Lane 1: DSPE-PEG2000-aptamer; Lane 2: complex of DSPE-PEG2000-aptamer-LNPs-RNAi; Lane 3: free aptamer

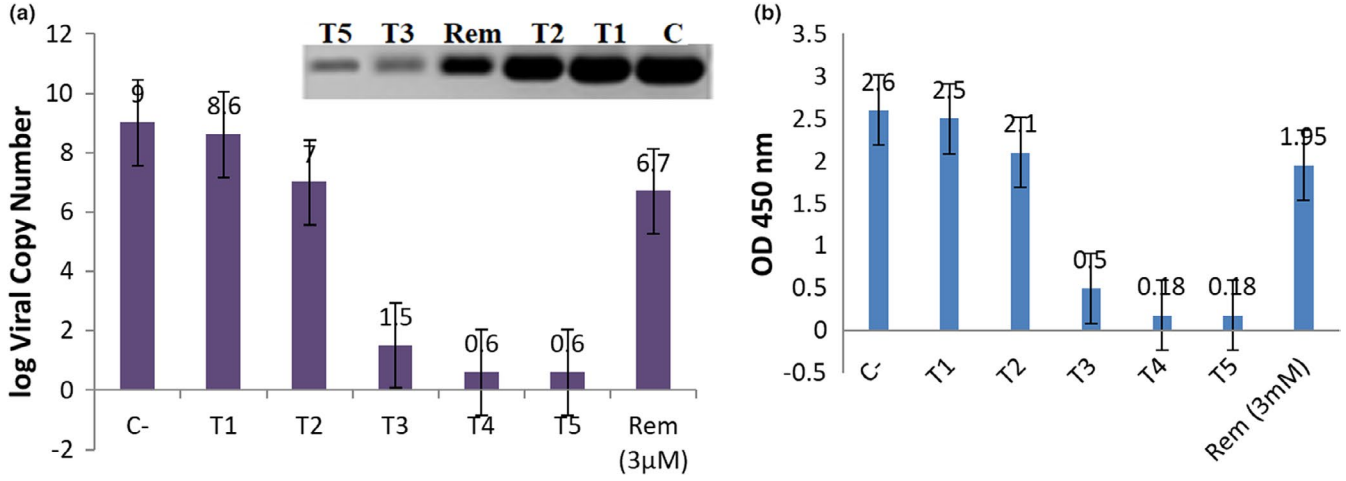

FIGURE 5 Comparison of antiviral activity of Apt-LNPs-RNAi and Remdesivir against SARS-CoV-2 in human lung cell lines. (a) q-PCR and semi-quantitative RT-PCR analysis of virus load in cell culture subjected to candidate antiviral Apt-LNPs-RNAi. C-: Negative control or no antiviral treatment, T1-T5 are liposome containing different concentration of aptamer and RNAi: T1: Apt 50 μM + 40 nM RNAi, T2: 60 μM Apt + 50 nM RNAi, T3: 70 μM Apt + 60 nM RNAi, T4: 90 μM Apt + 70 nM RNAi, T5: 100 μM Apt + 80 nM RNAi and Rem: 3 μM Remdesivir. The y-axis indicates the log viral RNA copy number. Bars represent standard error between samples ($n = 34$). Semi-quantitative RT-PCR (gel picture at the top of the chart) and q-PCR analyzes confirmed the significant decreases in the viral copy number from 9 copies to 0.6 copy by incubating cell culture with Apt-LNPs-RNAi. (b) Enzyme-linked immunosorbent assay (ELISA) results of HBE135-E6E7-harvested supernatant at OD 450 nm. The results are expressed as optical density (OD). The ELISA results showed that with the use of Apt-LNPs-RNAi, SARS-CoV-2 quantity decreased from 2.6 to 0.18 OD [Colour figure can be viewed at wileyonlinelibrary.com]

number of SARS-CoV-2 copies by 50%. Semi-quantitative RT-PCR and q-PCR analyzes (Figure 5a) confirmed the significant decreases in the viral copy number from 9 copies to 0.6 copies by incubating cell culture with Apt-LNPs-RNAi (concentration 90 μM Apt+70 nM RNAi). In addition, the ELISA results showed that with the use of Apt-LNPs-RNAi, SARS-CoV-2 quantity decreased from 2.6 to 0.18 OD.

TABLE 4 Results of the biochemistry and hematology tests at the indicated days of the Apt-LNPs-RNAi administration

Days after inpatient admission					
	First day Before treatment (Step A radiology)	**Post 3 days Apt-LNPs-RNAi (Step B radiology)**	**Post 6 days Apt-LNPs-RNAi (Step C radiology)**	**Post 20 days**	**Normal range**
WBC	9.93	8.7	8.6	5.3	3.5–10.5 (×10(3)/mcL)
Neutrophil count	8.46	7.8	6	5.6	4.44 (×10(3)/mcL)
Lymphocyte count	3.62				(0.8–5.0) (×10(3)/mcL)
Alanine transaminase	61	58	50	46	10–45 IU/L
Alkaline phosphatase	105.49	10.1	95.4	50	30–130 IU/L
Cytokines (IL-6)	22.1	22	19.1	16	≤18 mg/L
Procalcitonin	10	6.2	2	0.1	0 to 0.05 (μg/L)
Urea	11.60	10.3	8	6.7	3.2–7.4 mmol/L
Troponin	20	16	5	0.6	0 and 0.4 ng/mL
C-reactive protein (CRP)	50.6	20	9	6	0–5 mg/L
Creatinine	7.8	4	1.9	0.9	0.8 mg/dL
Total bilirubin	11.4				0–21 μmol/L
Lactate dehydrogenase (LD)	600	430	300	230	90–235 IU/L
Albumin	39	46.3	52	49.6	34 to 54 g/L

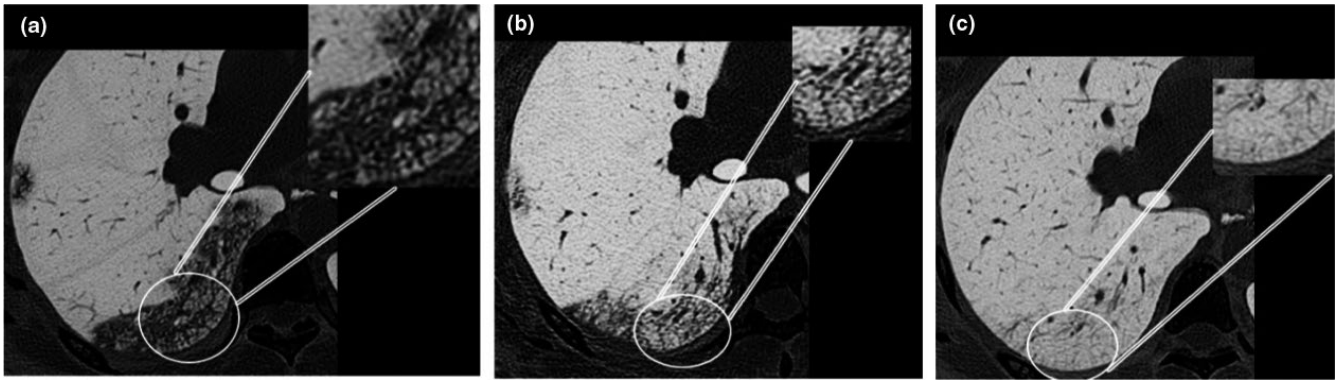

FIGURE 6 An axial CT scan image in lung. (a) Chest CT scan image before Apt-LNPs-RNAi treatment on the first day, in which the extent of the ground-glass opacification is propagated and expanded and almost severe bronchitis is seen. (b) A CT scan of the chest on day 3 of the treatment, in which bronchitis or ground-glass opacification are seen with lower densities. In image (c), which is the CT scan of the patient on day 6, the ground-glass opacification are almost scattered and parenchymal tissue is seen

3.6 | Clinical assessment of the response to Apt-LNPs-RNAi

A patient admitted to the hospital with severe coronary symptoms such as fever and shortness of breath was treated. Results of q-PCR confirmed that our patient was positive SARS-CoV-2.

Different clinical tests demonstrated a rising IL-6, CRP, WBC, Neutrophil, Lymphocyte, Alanine transaminase, Alkaline phosphatase, Procalcitonin, Urea, Troponin, Creatinine, Total bilirubin, Lactate dehydrogenase (LD), and a decreasing Albumin (Table 4). Moreover, Chest CT scan results (Figure 6) demonstrated radiological SARS-CoV-2 features such as ground-glass opacity (GGOs).

A soft mist inhaler was used for inhalation of Apt-LNPs-RNAi, 10 mg Apt-LNPs-RNAi nebulized/day for six days, and chest CT scan and biochemical tests recorded daily. Three days after Apt-LNPs-RNAi administration there was an improvement in consolidation and ground-glass opacity. On the sixth day of treatment, following a relapse of fever and other symptoms, further improvement in the ground-glass opacification (GGOs) was observed.

The results of biochemical and hematological tests in coordination with radiographs approved the SARS-CoV-2 healing process, so that the amount of biomarkers approached the standard values over time (Table 4).

4 | DISCUSSION

The rapid pandemic of SARS-CoV-2 has posed a great threat to the social health system, economy, and these influences continue for a longer time. We need to learn the pandemic logic of SARS-CoV-2 and investigate the unknown microorganisms such as viruses in nature in advance to make early warning. As the global pandemic worsens, specific anti- SARS-CoV-2 drugs, safe and effective vaccines and antibodies are in urgent need. Currently, A small number of Corona vaccines have been reported, which their true efficacy and safety are still unclear. During the SARS-CoV-2 pandemic, researchers are investigating a variety of possible treatments. According to the pathological sign and symptoms and clinical phases of SARS-CoV-2, the classes of administrated drugs are inflammation inhibitors such as antirheumatic drugs, heparins, plasma, and nonspecific antiviral agents. Neutralizing monoclonal or polyclonal antibodies are expected effective for SARS-CoV-2 infection, but their covering rates, production scales, and costs are still questions. Vaccine development for SARS-CoV-2 also faces difficulties such as ineffectiveness due to virus mutation. Because of our incomplete finding on the SARS-CoV-2 world and the host interaction, there is no one satisfactory antiviral agent available till now. The designed antiviral drug should recognize viral proteins, or segments of genomes, that can be disabled. These targeted segments of virus should be as *nonhomologous* sequences or unlike any molecules in humans as possible, to reduce the likelihood of side effects. Most of the SARS-CoV-2 structural proteins, such as N protein, showed no significant difference in protein sequence and architecture between SARS-CoV-2 and other known Covids. The S protein, especially the RBD segment, of SARS-CoV-2 is responsible for binding the human cell-surface receptor known as hACE2 during cell entry. The primary role of the SARS-CoV-2 nucleocapsid (N) protein is to pack viral genome into ribonucleoprotein complex. Nucleocapsid protein (N) is highly conserved among phylogenetically distant Covid strains and targeting of this protein can overcome drug resistance.

Herein, we targeted the N protein of SARS-CoV-2 to identify promising RNAi-based antiviral candidates. Knowing the role and importance of S and N proteins in SARS-CoV-2 pathogenesis, we hypothesized that by

specifically targeting these two proteins, a specific corona antivirus could be produced. Naked siRNA molecules are generally digested by ribonucleases, and due to their negative charge, RNAi entry into the host cells is also hampered that makes necessary the use of a suitable delivery system. Lipid nanoparticles are one of the best drug delivery systems for the clinical application of RNAi due to their simplicity of production, relative safety, and enhanced protection and payload of encapsulated RNAi. Moreover, LNPs can be functionalized using specific aptamers to reach target cells. Aptamers are highly useful in producing theranostic drugs and generic drugs for certain diseases like Alzheimer's disease (Qu et al., 2017). They bind to diverse targets like nucleic acids, lipids, small organic compounds, proteins, and even entire microorganisms. Specific DNA/RNA aptamers can be used to interfere in the viral replication cycle and hamper its penetration into host cells. Previous studies have reported the utilization of aptamers as a diagnostic tool or treatment in viral infections, for example, HBV (Hepatitis B Virus), HIV (Human Immunodeficiency Virus), HCV (Hepatitis C Virus), H5N1 avian influenza, SARS (Severe Acute Respiratory Syndrome) and recently Ebola (Li et al., 2018; Wandtke et al., 2015). Moreover, due to superior target-specific biophysical binding properties, aptamers cause decreased off-target toxicity effects. Therefore, research for aptamer-based diagnostic tools, aptamer-based drugs and drug-carriers are expanding fast. Here, we used a combination of three basic strategies including the antiviral effect of aptamer on the S protein, the inhibitory effect of RNAi on the N protein, and advantages of specific drug delivery with the help of aptamer-functionalized nanocarrier to combat SARS-CoV-2 in the best possible way. In this study SARS-CoV-2 RBD was cloned in *E. Coli*, purified, and used as the aptamer selection target. Influenza A Virus Nucleoprotein (INP) was used as negative controls from the fourth round of SELEX. After nine rounds of screening, the sequences with the highest copy number were considered as candidate aptamers. The K_D results demonstrated that Apt1 with K_D values of 0.290 ± 0.07 μM had the best affinities toward the RBD than the other sequences. In comparison with previous reported studies, Apt1 has an appropriate affinity to the target (Weisshoff et al., 2020). Therefore, Apt1 was used for antiviral assay and RNAi delivery. We proposed that aptamer-modified LNPs containing RNAi molecules were stably formulated by PEGylation. The first PEGylation of LNPs provided sufficient cationic charges to complex with anionic RNAi molecules, as previously suggested by Kim et al. (2017). The second addition of PEG-aptamer conjugates made the LNPs surface negative, which would provide adequate enhanced permeability and retention effects (Ho et al., 2013 and Ngoune et al., 2016). This electro-negativity of the LNPs surface is a critical environment to present the proper orientation of negatively charged aptamers exposed outward. In addition, the high aggregate and density of PEG molecules protected the Apt-LNPs from being digested by serum enzymes, which would be significant factor during clinical application. Results of gel retardation assay indicated considerable retardation of RNAi molecules due to coupling with cationic lipids an P/N ratio of 1:6 (Figure 4a). Digestion of siRNA with RNAse A indicated that Ap-LNPs could effectively protect about 75% of the incorporated siRNA molecules from cellular endonucleases degradation (Figure 4b). As shown in Figure 4c, RBD aptamers were efficiently conjugated to DSPE-PEG2000-maleimide, and then aptamer-DSPE-PEG2000 was successfully attached to the prepared liposomes-RNAi. Compared to other studies (Ho et al., 2013; Kim et al., 2017; Rejman et al., 2004), our data show that the designed drug carrier has appropriate standards for clinical use. Anti SARS-CoV-2 assessment of Apt-LNPs-RNAi was performed in lung cell lines (HBE135-E6E7). We performed the isolation of SARS-CoV-2 in Vero E6 cells, which led to the adaptation of SARS-CoV-2 with increased infectivity and cytopathic effect titers in Vero E6 cells. Thus, the adapted isolated virus from Vero E6 cells permits culture across additional human cell lines such as lung cell lines (HBE135-E6E7), and an efficient tool for the screening of putative SARS-CoV-2 antiviral agents. The virus supernatant derived from Vero E6 passage was used to inoculate lung cell lines, and the antiviral susceptibility of SARS-CoV-2 for Apt-LNPs-RNAi was determined by measuring the reduction of the SARS-CoV-2 copy number in culture supernatants using q-PCR and ELISA. We examined the antiviral effects of Aptamer-LNPs and LNPs-RNAi in two separate experiments. Although Aptamer-LNPs and LNPs-RNAi separately showed antiviral effects (Figures S1–S3), their combination showed better antiviral effects in a synergistic manner (Figure 5). As shown in the Figure 5a,b, q-PCR, semi-quantitative RT-PCR and ELISA analyzes indicated that the combination of Apt-LNPs-RNAi had antiviral effects, so that the combinations of 90 μM Apt and 70 nM RNAi (Figure 5: T4) showed the best anti SARS-CoV-2 effect. Compared to the negative control, the designed Apt-LNPs-RNAi reduced the amount of virus by 15 folds, and it performed better anti SARS-CoV-2 effect than Remdesivir (as a positive control: which only reduced the virus titer by 1.3 folds). Antiviral RNAi treatment has many advantages over vaccines and conventional anti-viral drugs, because; a little concentration of RNAi molecule is enough to decrease viral RNA load, and it has rapid activity with high specificity and efficiency at different stages of viral infection (Javaria et al., 2020). Respiratory syncytial virus was

successfully inhibited using RNAi. Similarly, intranasally administered RNAi was indicated to reduce or inhibit the viral activity of para-influenza virus up to 99% (Bitko et al., 2005). Intranasal administration of two RNAi duplexes targeting ORF1b and spike coding regions of SARS-CoV were resulting in diminished SARS-CoV titer, reduced fever, and reduced diffuse alveoli damage (Ge et al., 2021). Appropriately aptamer-modified nanoparticles provide immunologically inert-surfaces contact with the human system in addition to possessing the high retention efficiency and permeability to enhance their deposition and efficacy in targeted tissues. Previous studies have reported that lipid nanocarriers protect RNAi molecules from serum nucleases, prolong their perdurability and enhance their targeting (Torrecilla et al., 2014 and Yaoying et al., 2017). The aerosol-based delivery of plasmid DNA using cationic liposomes was reported for the delivery of siRNA by Thomas and co-workers 2007 (Arulmuthu et al., 2007). A lipid-based nanodevice has been reported for delivery of RNAi molecules into lung epithelium to treat lung metastasis. The nanodevice is guided to the lungs by surface functionalization with GALA-peptide, which binds with the sialic acid chains on the lung endothelium (Javaria et al., 2020). A lipid nanocarrier has also been utilized for pulmonary delivery of RNAi (Arulmuthu et al., 2007). Here, applied aptamer in the nanocarrier has two important functions. First, it can deliver the drug (RNAi) to the surface of epithelial cells. Second, by binding to the SARS-CoV-2 spike protein, it inhibits the virus entrance into cells.

5 | CONCLUSION

In conclusion, we optimized an aptamer against SARS-CoV-2 RBD. The selected aptamer is ideal for SARS-CoV-2 RBD targeting due to its high affinity (K_D values 0.29 μM). It seems that the aptamer and ACE2 have a competitive relationship. Aptamer strands are binding to spike protein hamper virus packaging and inhibit SARS-CoV-2 attachment to human cell receptors. Therefore, this aptamer is a candidate for preventing the SARS-CoV-2 from infecting human cells and will be increasingly applied as antiviral therapeutics or for targeting drug delivery. Aptamer-LNPs-RNAi achieved better gene silencing and antiviral action when compared to just aptamer or just RNAi. Clinical case study demonstrated that inhalation of 10 mg Apt-LNPs-RNAi nebulized/day for six days resulted in an improvement in consolidation and ground-glass opacity on the sixth day of treatment. Our findings suggest the treatment of SARS-CoV-2 infection through self-inhalation of Aptamer-LNPs-RNAi.

ACKNOWLEDGMENTS

We thank the Rojava-Ministry of Health for laboratory assistance and the clinical case study. Moreover, we thank the Institute of Science and Modern Technology, Rojava University for their partial financial supports.

CONFLICT OF INTEREST

The authors declare that there are no conflicts of interests.

AUTHOR CONTRIBUTIONS

Saify H. designed the research and wrote the manuscript, Saify H. and Amini M. performed the research, and Serwet D. analyzed the research. All authors reviewed the manuscript.

DATA AVAILABILITY STATEMENT

All data are available from the authors upon request.

ORCID

Haidar Saify Nabiabad https://orcid.org/0000-0001-7364-9001

REFERENCES

Arulmuthu, E. R., Williams, D. J., Baldascini, H., Versteeg, H. K., & Hoare, M. (2007). Studies on aerosol delivery of plasmid DNA using a mesh nebulizer. *Biotechnology and Bioengineering*, *98*(5), 939–955. https://doi.org/10.1002/bit.21493

Ayal, G., Noam, A., Guilhem, F., Wolf, Y. I., Zhang, F., & Kooninet, E. V. (2020), Genomic determinants of pathogenicity in SARS-CoV-2 and other human coronaviruses. bioRxiv. Preprint. 2020 Apr 9.

Bhandare, V., & Ramaswamy, A. (2016). Structural dynamics of human argonaute2 and its interaction with siRNAs designed to target mutant tdp43. *Advances in Bioinformatics*, *2016*, 8792814. https://doi.org/10.1155/2016/8792814

Bitko, V., Musiyenko, A., Shulyayeva, O., & Barik, S. (2005). Inhibition of respiratory viruses by nasally administered siRNA. *Nature Medicine*, *11*, 50–55. https://doi.org/10.1038/nm1164

Chan, J.-W., Yuan, S., Kok, K.-H., To, K.-W., Chu, H., Yang, J., Xing, F., Liu, J., Yip, C.-Y., Poon, R.-S., Tsoi, H.-W., Lo, S.-F., Chan, K.-H., Poon, V.-M., Chan, W.-M., Ip, J. D., Cai, J.-P., Cheng, V.-C., Chen, H., ... Yuen, K.-Y. (2020). A familial cluster of pneumonia associated with the 2019 novel coronavirus indicating person-toperson transmission: a study of a family cluster. *Lancet*, *395*, 514–523. https://doi.org/10.1016/S0140-6736(20)30154-9

Chowdhury, F. T., Shohan, M. U. S., Islam, T., Mimu, T. T., & Palit, P. (2019). A therapeutic approach against leishmania donovani by predicting RNAi molecules against the surface protein, gp63. *Current Bioinformatics*, *14*, 541–550. https://doi.org/10.2174/1574893613666180828095737

Chowdhury, U. F., Sharif Shohan, M. U., Hoque, K. I., Beg, M. A., Sharif Siam, M. K., & Moni, M. A. (2021). A computational approach to design potential siRNA molecules as a prospective tool for silencing nucleocapsid phosphoprotein and surface glycoprotein gene of SARS-CoV-2. *Genomics*, *113*(1), 331–343. https://doi.org/10.1016/j.ygeno.2020.12.021

Cook, A. B., & Decuzzi, P. (2021). *Harnessing endogenous stimuli for responsive materials in theranostics*. ACS Nano. Article ASAP.

Ge, X., Chen, L., Zhao, B. O., & Yuan, W. (2021). Rationale and application of PEGylated lipid-based system for advanced target delivery of siRNA. *Frontiers in Pharmacology*, *11*, 598175. https://doi.org/10.3389/fphar.2020.598175

Geng, M., Li, X., Peng, Y., Meng, L., & Lu, S. (2020). Molecular immune pathogenesis, diagnosis of COVID-19. *Journal of Pharmaceutical Analysis*, *10*(2), 102–108. https://doi.org/10.1016/j.jpha.2020.03.001

Ho, E. A., Osooly, M., Strutt, D., Masin, D., Yang, Y., Yan, H., & Bally, M. (2013). Characterization of long-circulating cationic nanoparticle formulations consisting of a two-stage PEGylation step for the delivery of siRNA in a breast cancer tumor model. *Journal of Pharmaceutical Sciences*, *102*, 227–236. https://doi.org/10.1002/jps.23351.

Kim, M. W., Yeon Jeong, H., Kang, S. J., Choi, M. J., & Myoung, Y. Y. (2017). Cancer-targeted nucleic acid delivery and quantum dot imaging using EGF receptor aptamerconjugated lipid nanoparticles. *SCIenTIfIC REPOrTS*, *7*, 9474. https://doi.org/10.1038/s41598-017-09555

Lan, W., Lin-Ping, W., Jingya, W., Jin, S., Zhonggui, H., Rodríguez-Rodríguez, C., Saatchi, K., Dailey, L. A., Häfeli, U. O., Cun, D., & Yang, M. (2021). Poly(lactide-co-glycolide) nanoparticles mediate sustained gene silencing and improved biocompatibility of siRNA delivery systems in mouse lungs after pulmonary administration. *ACS Applied Materials & Interfaces*, *13*(3), 3722–3737. https://doi.org/10.1021/acsami.0c21259

Levanova, A., & Poranen, M. M. (2018). RNA interference as a prospective tool for the control of human viral infections. *Frontiers in Microbiology*, *9*, 2151. https://doi.org/10.3389/fmicb.2018.02151.

Li, B., & Webster, T. J. (2018). Bacteria antibiotic resistance: New challenges and opportunities for implant-associated orthopedic infections. *Journal of Orthopaedic Research*®,*36*(1), 22–32.

Lysebetten, D., Malfanti, A., Deswarte, K., Koynov, K., Golba, B., Ye, T., Zhong, Z., Kasmi, S., Lamoot, A., Chen, Y., Van Herck, S., Lambrecht, B. N., Sanders, N. N., Lienenklaus, S., David, S. A., Vicent, M. J., De Koker, S., & De Geest, B. G. (2021). Lipid-polyglutamate nanoparticle vaccine platform. *ACS Applied Materials & Interfaces*, *13*(5), 6011–6022. https://doi.org/10.1021/acsami.0c20607

Ngoune, R., Peters, A., von Elverfeldt, D., Winkler, K., & Pütz, G. (2016). Accumulating nanoparticles by EPR: A route of no return. *Journal of Controlled Release*, *238*, 58–70. https://doi.org/10.1016/j.jconrel.2016.07.028

Qu, J., Yu, S., Zheng, Y., Zheng, Y., Yang, H., & Zhang, J. (2017). Aptamer and its applications in neurodegenerative diseases. *Cellular and Molecular Life Sciences*, *74*, 683–695. https://doi.org/10.1007/s00018-016-2345-4

Ramirez, S., Fernandez-Antuneza, C., Long, V., Phama, A., Ryberg, L. A., Feng, S., Pedersen, M. S., Mikkelsen, L. S., Belouzard, S., Dubuisson, J., Sølund, C., Weis, N., Gottwein, J. M., Fahnøe, U., & Bukh, J. (2020). Efficient culture of SARS-CoV-2 in human hepatoma cells enhances viability of the virus in 2 human lung cancer cell lines permitting the screening of antiviral compounds. *bioRxiv*. Preprint 2020. https://doi.org/10.1101/2020.10.04.325316.

Rejman, J., Wagenaar, A., Engberts, J. B., & Hoekstra, D. (2004). Characterization and transfection properties of lipoplexes stabilized with novel exchangeable polyethylene glycol-lipid conjugates. *Biochimica Et Biophysica Acta*, *1660*, 41–52. https://doi.org/10.1016/j.bbamem.2003.10.011.

Saify Nabiabad, H., Piri, K., & Amini, M. (2018). Expression of active chimeric-tissue plasminogen activator in tobacco hairy roots, identification of a DNA aptamer and purification by aptamer functionalized-MWCNTs chromatography. *Protein Expression and Purificationm*, *152*, 137–145. https://doi.org/10.1016/j.pep.2016.02.004

Saw, P. E., & Song, E. W. (2019). siRNA therapeutics: a clinical reality. *Science China Life Sciences*, *63*(4), 485–500. https://doi.org/10.1007/s11427-018-9438-y

Song, F., Shi, N., Shan, F., Zhang, Z., Shen, J., Lu, H., Ling, Y., Jiang, Y., & Shi, Y. (2020). Emerging 2019 novel coronavirus (2019-nCoV) pneumonia. *Radiology*, *295*, 210–217. https://doi.org/10.1148/radiol.2020200274.

Song, Y., Song, J., Wei, X., Huang, M., Sun, M., Zhu, L., Lin, B., Shen, H., Zhu, Z., & Yang, C. H. (2021). Discovery of aptamers targeting the receptor-binding domain of the SARS-CoV-2 spike glycoprotein. *Analytical Chemistry*, *92*(14), 9895–9900. https://doi.org/10.1021/acs.analchem.0c01394

Terada, T., Jayesh, A. K., Ariel, H., Sam, C. H., van der Meel, R., Yi, C. Y., & Cullis, P. R. (2021). Characterization of lipid nanoparticles containing ionizable cationic lipids using design-of-experiments approach. *Langmuir*, *37*(3), 1120–1128. https://doi.org/10.1021/acs.langmuir.0c03039

Torrecilla, J., Rodríguez-Gascón, A., & Solinís, M. Á. (2014). Lipid nanoparticles as carriers for RNAi against viral infections: current status and future perspectives. *Biomed Research International*, *2014*:161794. https://doi.org/10.1155/2014/161794

Ullah, A., Qazi, J., Rahman, L., Kanaras, A. G., Khan, W. S., Hussain, I., & Rehman, A. (2020). Nanoparticles-assisted delivery of antiviral-siRNA as inhalable treatment for human respiratory viruses: A candidate approach against SARS-COV-2. *Nano Select*, *1*, 612–621. https://doi.org/10.1002/nano.202000125

Walls, A. C., Tortorici, M. A., Bosch, B. J., Frenz, B., Rottier, P. J. M., DiMaio, F., Rey, F. A. & Veesler, D. (2016). Cryo-electron microscopy structure of a coronavirus spike glycoprotein trimer. *Nature*, *531*, 114–117. https://doi.org/10.1038/nature16988

Wandtke, T., Woźniak, J., & Kopiński, P. (2015). Aptamers in diagnostics and treatment of viral infections. *Viruses*, *7*, 751–780. https://doi.org/10.3390/v7020751.

Weisshoff, H., Krylova, O., Nikolenko, H., Düngen, H.-D., Dallmann, A., Becker, S., Göttel, P., Müller, J., & Haberland, A. (2020). Aptamer BC 007 - Efficient binder of spreading-crucial SARS-CoV-2 proteins. *Heliyon*, *6*, e05439. https://doi.org/10.1016/j.heliyon.2020.e05421.

Westerbeck, J. W., & Machamer, C. E. (2019). The infectious bronchitis coronavirus envelope protein alters golgi pH toprotect the spike protein and promote the release of infectious virus. *Journal of Virology*, *93*, e00015–e00019.

Yaoying, W., Adam, E., & Theresa, M. (2017). Reineke. lipophilic polycation vehicles display high plasmid DNA delivery to multiple cell types. *Bioconjugate Chemistry*, *28*(8), 2035–2040. https://doi.org/10.1021/acs.bioconjchem.7b00306

Youngren, S. R., Gandhi, N. S., España-Serrano, L., & Chougule, M. B. (2016). Aerosol delivery of siRNA to the lungs. Part 1: rationale for gene delivery systems. *KONA Powder Part J*, *33*, 63–85. https://doi.org/10.14356/kona.2016014

Zheng, B., Guan, Y., Tang, Q., Du, C., Xie, F. Y., He, M.-L., Chan, K.-W., Wong, K.-L., Lader, E., Woodle, M. C., Lu, P. Y., Li, B., & Zhong, N. (2004). Prophylactic and therapeutic effects of small interfering RNA targeting SARS-coronavirus. *Antiviral Therapy*, *9*, 365–374.

Zhou, P., Yang, X.-L., Wang, X.-G., Hu, B., Zhang, L., Zhang, W., Si, H.-R., Zhu, Y., Li, B., Huang, C.-L., Chen, H.-D., Chen, J., Luo, Y., Guo, H., Jiang, R.-D., Liu, M.-Q., Chen, Y., Shen, X.-R., Wang, X. I., ... Shi, Z.-L. (2020). A pneumonia outbreak associated with a new coronavirus of probable bat origin. *Nature*, *579*, 270–273. https://doi.org/10.1038/s41586-020-2012-7

SUPPORTING INFORMATION

Additional supporting information may be found in the online version of the article at the publisher's website.

How to cite this article: Saify Nabiabad, H., Amini, M., & Demirdas, S. (2022). Specific delivering of RNAi using Spike's aptamer-functionalized lipid nanoparticles for targeting SARS-CoV-2: A strong anti-Covid drug in a clinical case study. *Chemical Biology & Drug Design*, 99, 233–246. https://doi.org/10.1111/cbdd.13978